



Sensitive sandwich immunoassay based on single particle mode inductively coupled plasma mass spectrometry detection

Rui Liu^{a,b}, Zhi Xing^a, Yi Lv^b, Sichun Zhang^a, Xinrong Zhang^{a,*}

^a Key Laboratory for Atomic and Molecular Nanosciences of Ministry of Education (MOE), Department of Chemistry, Tsinghua University, Tsinghua Yuan, Beijing 100084, PR China

^b Key Laboratory of Green Chemistry and Technology of Ministry of Education (MOE), College of Chemistry, Sichuan University, Chengdu 610064, PR China

ARTICLE INFO

Article history:

Received 20 June 2010

Received in revised form 15 August 2010

Accepted 24 August 2010

Available online 27 September 2010

Keywords:

Inductively coupled plasma mass spectrometry (ICP-MS)

Sandwich immunoassay

Single particle

Time resolved analysis

Colloidal gold

IgG

ABSTRACT

A sensitive sandwich type immunoassay has been proposed with the detection by inductively coupled plasma mass spectrometry (ICP-MS) in a single particle mode (time resolved analysis). The signal induced by the flash of ions ($^{197}\text{Au}^+$) due to the ionization of single Au-nanoparticle (Au-NP) label in the plasma torch can be measured by the mass spectrometer. The frequency of the transient signals is proportional to the concentration of Au-NPs labels. Characteristics of the signals obtained from Au-NPs of 20, 45 and 80 nm in diameters were discussed. The analytical figures for the determination of Au-labeled IgG using ICP-MS in conventional integral mode and single particle mode were compared in detail. Rabbit-anti-human IgG was used as a model analyte in the sandwich immunoassay. A detection limit (3σ) of 0.1 ng mL^{-1} was obtained for rabbit-anti-human IgG after immunoreactions, with a linear range of $0.3\text{--}10 \text{ ng mL}^{-1}$ and a RSD of 8.1% (2.0 ng mL^{-1}). Finally, the proposed method was successfully applied to spiked rabbit-anti-human IgG samples and rabbit-anti-human serum samples. The method resulted to be a highly sensitive ICP-MS based sandwich type immunoassay.

© 2010 Elsevier B.V. All rights reserved.

1. Introduction

Element-tagged immunoassay with inductively coupled plasma mass spectrometry (ICP-MS) detection has been extensively studied and well established in the past few years [1–5]. The advantages of using ICP-MS in immunoassays with element tagging include low detection limits, large dynamic range, multiplexing potential, good spectral resolution and free of radioactive isotope or toxic enzyme substrate reagents. In addition, this technique receives low biological matrix effects. Methods for the determination of biological analytes such as small biomolecule [6,7], protein [8–16], DNA [17], bacteria [18] and even cell [19–21] have been proved to be successful by several groups. The multiplexed detection ability has also been fully demonstrated by using this ICP-MS based immunoassay [8,22–24]. Besides, as an imaging tool, laser ablation (LA)-ICP-MS was proposed for the multi-analytes imaging in tissue section [25,26], protein microarray [24] and western blot membrane [27,28].

Previously, we described a single particle mode ICP-MS based immunoassay for α -fetoprotein [29], as enlightened from the spark of the single nanoparticle analysis with ICP-MS [30]. The strategy tends to be a sensitive readout method for nanoparticle tags, which

is promising for applications in biological analysis. Nevertheless, the published work was mainly focused on the competitive type immunoassay, and had not fully illustrated the merits of the ICP-MS based single particle analysis. Sandwich type immunoassay, as a noncompetitive immunoassay, is arguably the most important immunoassay method and widely used to determine antigen concentrations in various endeavors including clinical diagnostics and biochemical studies [31–34]. Most sandwich immunoassays work in solid-phase where microwells or tubes are served as carriers of immunoreagent. Sandwich type immunoassay methods have several advantages over competitive assays. For instance, they are generally 5–20 times more precise and sensitive than their respective competitive assays and less affected by nonspecific or specific interferences [35]. Therefore, sandwich type immunoassay methods for biomolecules usually do not require preliminary extraction and purification of the sample and thus use a lower sample volume than competitive assays. Furthermore, sandwich type immunoassays generally have a larger working range [35]. These merits suggest that sandwich type immunoassays for biosamples may be more suitable for clinical routine than competitive assays.

In this work, a highly sensitive sandwich immunoassay based on ICP-MS detection in single particle mode (time resolved analysis), with Au-nanoparticles (Au-NPs) serving as model tags, was proposed. The characteristics of the signals obtained from different sizes of Au-NPs were studied. To illustrate the performance of this single particle mode, the analytical figures of merits for the

* Corresponding author. Tel.: +86 10 6278 7678; fax: +86 10 6277 0327.
E-mail address: xrzhang@chem.tsinghua.edu.cn (X. Zhang).

Table 1
Working parameters of ICP-MS.

Parameters	Values
RF Power (W)	1200
Cool gas flow (L/min)	13
Auxiliary gas flow (L/min)	0.8
Nebulizer gas flow (L/min)	0.85
Sample uptake rate (mL/min)	0.5
Water stream flow rate (mL/min)	0.5
Torch	Shield torch
Cones	Nickel, HPI design
Data acquisition mode	Time resolved analysis (TRA)
Dwell time (ms)	10
TRA duration time (s)	60
Resolution	Standard
Analogue detector voltage (V)	2130
PC detector voltage (V)	3650

determination of Au-NPs labeled IgG using both modes (conventional integral mode and single particle mode) have been calculated for comparison. Characteristics of the signals obtained from Au-NPs labels, procedures to dissociate the antigen–antibody complex, effects of Au-NPs labels concentration and real sample analysis were discussed.

2. Experimental

2.1. Instrument

An X Series ICP-MS (Thermo Electron Co., Winsford, Cheshire, UK) was used throughout this work. The build-up of sample introduction manifold and the data acquisition parameters have been described previously [29], so only a brief account will be given here. The flow rates of the water stream and Au-NPs suspension were both 0.5 mL/min through a Y-shaped pipeline. Transient signals were recorded by ICP-MS in time resolved analysis (TRA) mode. With the dwell time of 10 ms, 6000 data points were provided during the time duration of 60 s. The working parameters of ICP-MS instrument were optimized and summarized in Table 1.

The morphologies of the Au-NPs were observed on a transmission electron microscope (TEM, Hitachi H-800) with an accelerating voltage of 100 kV. The enzyme-linked immunosorbent assay (ELISA) was performed with an ELISA reader (Tecan, Sunrise Remote/Touch Screen, Columbus plus, Austria).

2.2. Reagents and immunoreaction buffers

Deionized water with conductivity of $18.3 \text{ M}\Omega \text{ cm}^{-1}$ from a Milli-Q water purification system (Millipore Milford, MA, USA) was used in this work. Polystyrene 96-well microtiter plates (Nikon, Sino American Biotechnology Co., Beijing, China) were used to perform the immunoreactions. Human IgG, rabbit-anti-human IgG antibody (RAH IgG), goat-anti-rabbit IgG antibody (GAR IgG) and bovine serum albumin (BSA) were purchased from Beijing Biosynthesis Biotechnology Co. (Beijing, China). Colloidal Au-Nanoparticles and GAR IgG-colloidal Au conjugate (Au-GAR IgG) were synthesized in our laboratory. The buffers used were as follows: (A) coating buffer, 0.05 M carbonate/bicarbonate buffer solution, pH 9.6 (dissolve 2.601 g Na_2CO_3 and 3.437 g NaHCO_3 in 1 L deionized water); (B) blocking buffer: 3% (w/v, g mL^{-1}) BSA in 0.01 M sodium phosphate-buffered saline (PBS, dissolve 2.204 g $\text{Na}_2\text{HPO}_4 \cdot 12\text{H}_2\text{O}$, 0.600 g $\text{NaH}_2\text{PO}_4 \cdot 2\text{H}_2\text{O}$ and 8.766 g NaCl in 1 L deionized water), pH 7.4. The blocking solution was stored at 4°C and used within a week; (C) assay buffer, 0.01 M PBS containing 1% BSA (w/v), pH 7.4; and (D) washing buffer, 0.01 M PBS with 0.05% (v/v) Tween 20, pH 7.4.

2.3. Preparation of colloidal gold nanoparticles

Colloidal Au was prepared according to the literature with slight modification [33]. Briefly, after boiling 0.01% (m/v) $\text{HAuCl}_4 \cdot 4\text{H}_2\text{O}$ with an appropriate volume of 1% (m/v) trisodium citrate (namely, 50 mL 0.01% HAuCl_4 with 1.0, 0.50, 0.3 mL 1% trisodium citrate for 20, 45, and 80 nm average diameters of particles, respectively) in aqueous solution for 30 min, the resulted colloidal suspension was cooled and stored in 4°C . The average diameters of particles were 20, 45, and 80 nm, respectively, as confirmed by TEM (Fig. 1). The Au-NPs suspensions used for detection were serially diluted from the stock suspensions with pure water after sonicating for 5 min.

2.4. Preparation of colloidal gold–antibody conjugates

Antibody–colloidal conjugates were prepared according to the modification in the literature [33]. The GAR antibody (10% more than the minimum amount, which was determined using a flocculation test) was added to 1 mL of pH-adjusted colloidal Au suspension followed by incubation at room temperature for 1 h. The conjugates were centrifuged at 10,000 rpm for 10 min, and the

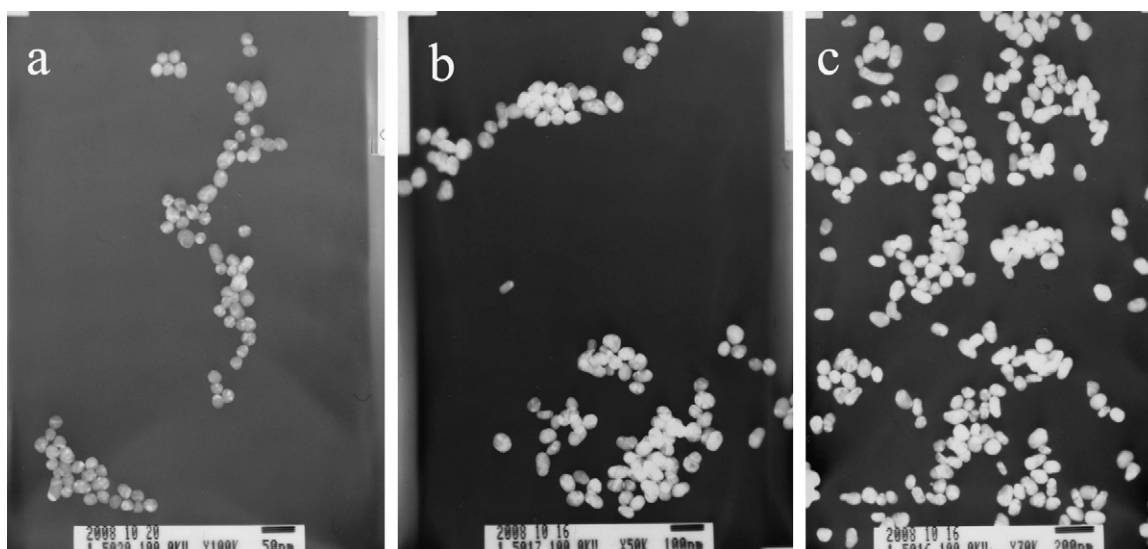


Fig. 1. TEM photograph of colloidal gold: (a) Au-NPs with 20 nm average diameter; (b) Au-NPs with 45 nm average diameter; and (c) Au-NPs with 80 nm average diameter.

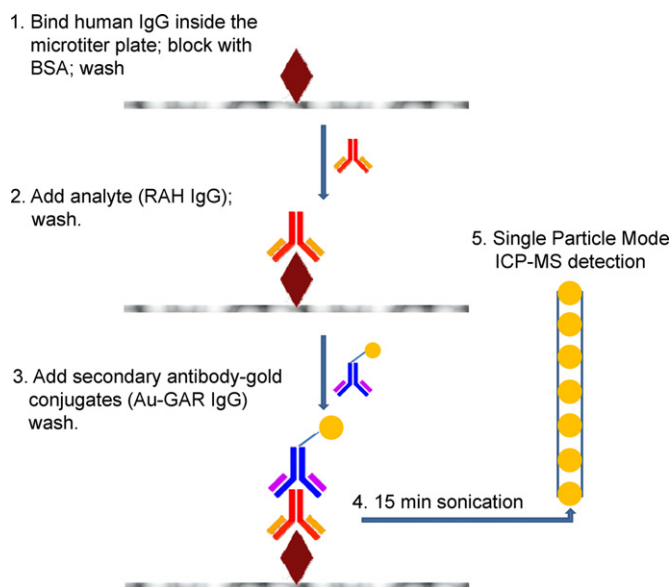


Fig. 2. Schematic diagram of the sandwich immunoassay for rabbit-anti-human IgG with Au-NP tags.

soft sediment was resuspended in 0.01 M PBS. A 1 mL suspension of Au-NP was tagged with 5 μg of GAR IgG. Addition of glycerol to a final concentration of 50% and BSA to a final concentration of 1% allows storage of the colloidal Au goat-anti-rabbit conjugates at -20°C for several months.

2.5. Immunoassay protocol

The immunoassay was conducted by following the typical procedure for sandwich type immunoreactions (Fig. 2). Initially, a polystyrene 96-well microtiter plate was coated using 200 μL of human IgG (diluted to 10 $\mu\text{g mL}^{-1}$ with coating buffer, pH 9.6) and incubated at 4°C overnight. The unbound antigen was washed away with washing buffer. After washing, the wells were incubated with blocking buffer for 1 h at 37°C . Afterward, the plate was washed three times. Series dilutions of RAH IgG antibodies with assay buffer were pipetted into the wells and incubated for 2 h at 37°C . Plates were washed six times followed by addition of colloidal Au-labeled GAR antibody (1:40 dilutions with assay buffer) to each well and incubated for 2 h at 37°C . After six times washing, a 200 μL aliquot of pure water was added to each well followed by 15 min sonication. Samples to be analyzed were diluted to 5 mL final volume and then introduced to the ICP-MS by peristaltic pump.

2.6. ELISA

The ELISA is a fundamental tool of clinical diagnosis for the detection of specific antigens or antibodies. In this work, ELISA was used as the standard method to validate the proposed method for the determination of RAH IgG serum samples. Briefly, the polystyrene wells were coated with human IgG and then blocked with blocking buffer, which procedures were the same as the proposed ICP-MS method. Afterward, 200 μL per well of a series of dilutions of RAH IgG serum samples were pipetted into the wells and incubated for 2 h at 37°C . After washing steps, 200 μL per well of horseradish peroxidase (HRP)-labeled GAR IgG (10 $\mu\text{g mL}^{-1}$) was added to the wells and incubated for 2 h at 37°C . After a final washing cycle, 200 μL per well of o-phenylenediamine (OPD) solution was added as the substrate to react with HRP. The reaction was stopped after 12 min by adding 50 μL 2 M H_2SO_4 and the absorbance was recorded at 490 nm.

3. Results and discussion

3.1. Characteristics of the signals obtained from Au-NPs

ICP-MS measurements were first carried out with 20, 45 and 80 nm gold colloids. Gold colloids were detected using the $^{197}\text{Au}^+$ signal whose isotopic abundance was 100%. Fig. 3a–d presents typical signals obtained from pure water, 20, 45 and 80 nm gold colloids as a function of time. Signals were recorded at every time slot of 10 ms. Currently, a record of 6000 data points was acquired during 60 s dwell time. The signal of pure water was of the order of 1 count per 10 ms while the signal of the particles ranged from say 3–30 counts per 10 ms for the 20 nm colloids, 5–100 counts per 10 ms for the 45 nm colloids, and 10–500 counts per 10 ms for the 80 nm colloids. The ICP-MS signal counts were apparently broad in distribution, because the particles measured were not strictly monodispersed and had size classes somewhat diverging from their mean size. Additionally, part of the ion cloud derived from a single particle in the plasma torch may occasionally escape from sampling cone during the ion transportation procedure. The 45 nm size of Au-NPs was chosen as optimum for single particle detection while considering both signal to noise ratio and the feasibility in bioapplications.

Fig. 3e shows the plot between the average intensity and colloid size. The experimental data directly followed a cubic trend which is in accordance with the theoretical value and a detection limit could be evaluated on a 3σ criteria. Linearity equation between average intensity and the cubic of particle diameter was calculated as Y (average intensity, counts per 10 ms) = $0.000366X$ (cubic of diameter, nm^3) + 0.707 and correlation coefficient (R) was found as 0.9992. In this study, the experimental conditions to detect gold colloids in a single particle analysis mode allow a size detection limit of around 15 nm (0.03 fg gold colloids).

3.2. Comparison of conventional integral mode and single particle mode ICP-MS for Au-labeled IgG detection

In order to illustrate the statistical differences in conventional integral mode and single particle mode ICP-MS detection, Au-labeled GAR IgG with an average Au particle size of 45 nm in diameter were investigated for its performance in ICP-MS with both detection modes. The original solution of Au-labeled GAR IgG was serially diluted to the concentration of 0.05 pg mL^{-1} GAR IgG by pure water.

Each Au-NP consists of a large number of gold atoms (2.8×10^6 gold atoms for 45 nm diameter particle), forming a heterogeneous solution with spatially-concentrated gold atoms suspended. The Au-NP was ionized separately in the plasma torch, forming a flash of ions that can be detected by mass spectrometer in TRA mode. Furthermore, the Au-NP as a single entity was not diluted by the nebulizing gas, thus remaining detectable even with extreme dilution and slight dispersion after atomization. On the contrary, while a solution of Au other than colloidal Au suspension was extremely diluted, the concentration of the analyte was not sufficient to produce detectable signals because of the sensitivity limitation of the present ICP-MS instrument, giving only the baseline noise similar to the signal of pure water.

Fig. 4a–i shows the signals recorded by ICP-MS in TRA mode for Au-GAR IgG suspension. As shown in the figure, the frequency of the transient signals is proportional to the concentration of Au-GAR IgG; the frequency of transient signals in 60 s decreased from 1466 ± 33 to 3 ± 1 when the suspension of Au-GAR IgG was diluted from 25 pg mL^{-1} to 0.05 pg mL^{-1} . Linear response of ICP-MS transient signal frequency to tagged proteins (Fig. 4j) indicates that ICP-MS in single particle mode could be employed for

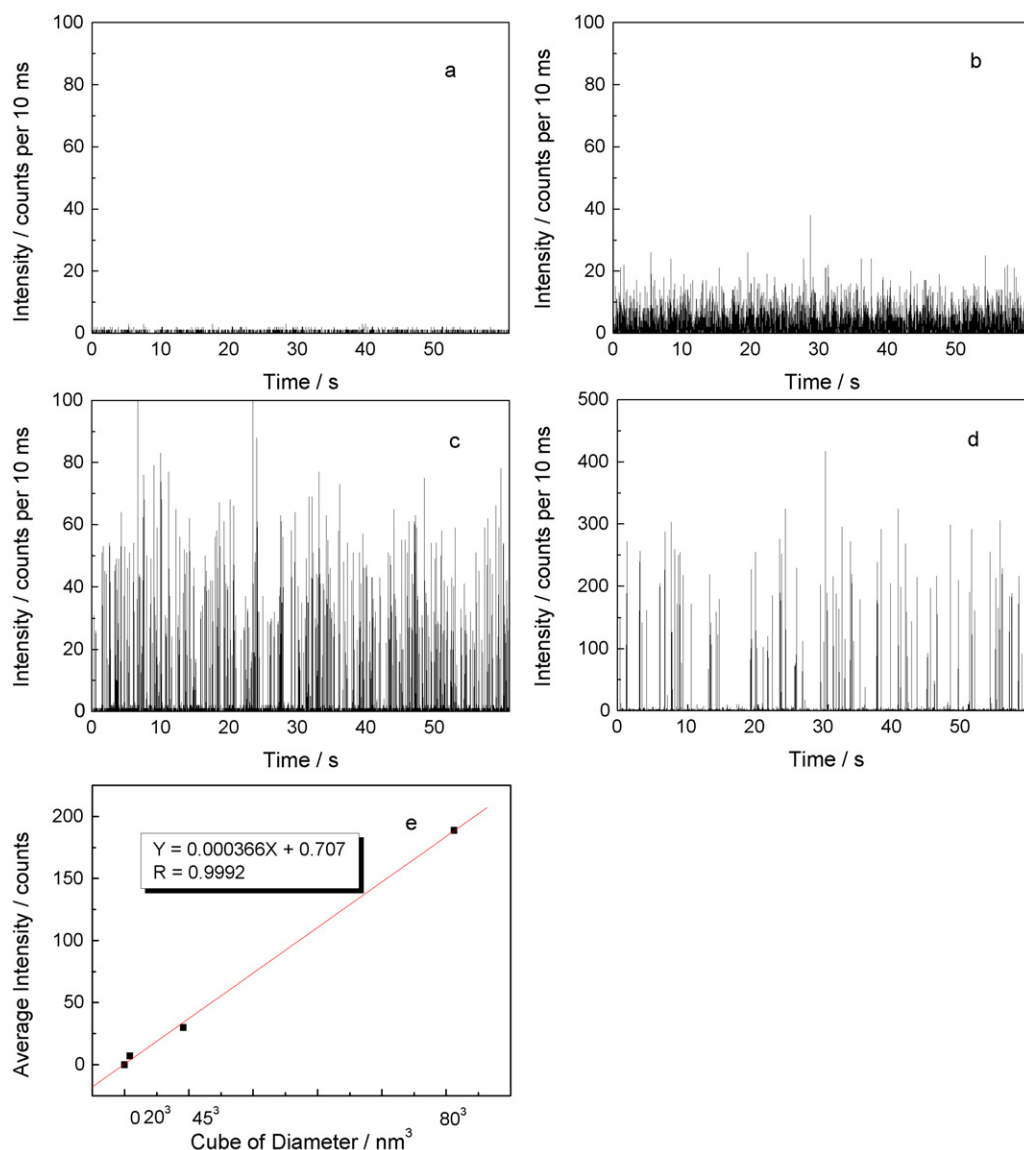


Fig. 3. Transient signals obtained from Au-NPs with different diameters by ICP-MS in TRA mode. (a) Pure water; (b) 10^6 times dilution (approximately 5.91×10^5 particles/mL) of Au-NPs suspension with 20 nm average size; (c) 10^6 times dilution (approximately 5.19×10^4 particles/mL) of Au-NPs suspension with 45 nm average size; (d) 10^6 times dilution (approximately 9.24×10^3 particles/mL) of Au-NPs suspension with 80 nm average size; and (e) the plot between the average intensity and cubic of average colloid diameter. Dwell time 10 ms; duration time: 60 s.

the determination of Au-labeled antibody, which is proportional to the analyte concentration in the sample after immunoassay.

The analytical figures of merits for the determination of Au-GAR IgG using conventional integral mode and single particle mode are both summarized in Table 2. With single particle mode ICP-MS detection, the limit of detection has about one order magnitude of improvement while comparing with conventional integral mode, which endows the possibility of developing highly sensitive immunoassay. However, the precision and linear range of TRA mode detection was slightly worse than conventional integral mode. In TRA mode, 6000 data points were acquired for each temporal profile within 60 s dwell time. In order to prevent Au particle from too dense to be recorded individually, a lower number of recorded pulse than 6000 should be guaranteed, usually, lower than 2000. It is somewhat detrimental to the linear range of the detection method. Obviously, the linear range of single particle mode will be expanded with the increase of sampling throughput (via decrease dwell time for each single particle or increase TRA duration time).

Possible aggregation of Au-NPs may explain the results of precision study, which caused an uncertainty in frequency counting.

3.3. Single particle mode ICP-MS based sandwich immunoassay for rabbit-anti-human IgG determination

The immunoreaction was conducted by using the procedure of sandwich type. The scheme is shown in Fig. 2. Human IgG was immobilized on the solid phase followed by using 3% BSA to block the nonspecific binding site. After the blocking step, the RAH IgG and colloidal Au-GAR IgG were added to form a sandwich complex of human IgG–RAH IgG–Au-GAR IgG.

The antigen–antibody complex can be dissociated under some extreme physiochemical conditions such as high temperature, low pH, and strong ionic strength. 1% HNO_3 was usually employed to dissociate the antigen–antibody complex from the solid surface after completion of the immunoassay [14]. However, extraordinarily high transient signals caused by the aggregation of Au-NPs was observed occasionally during the single particle mode detection in

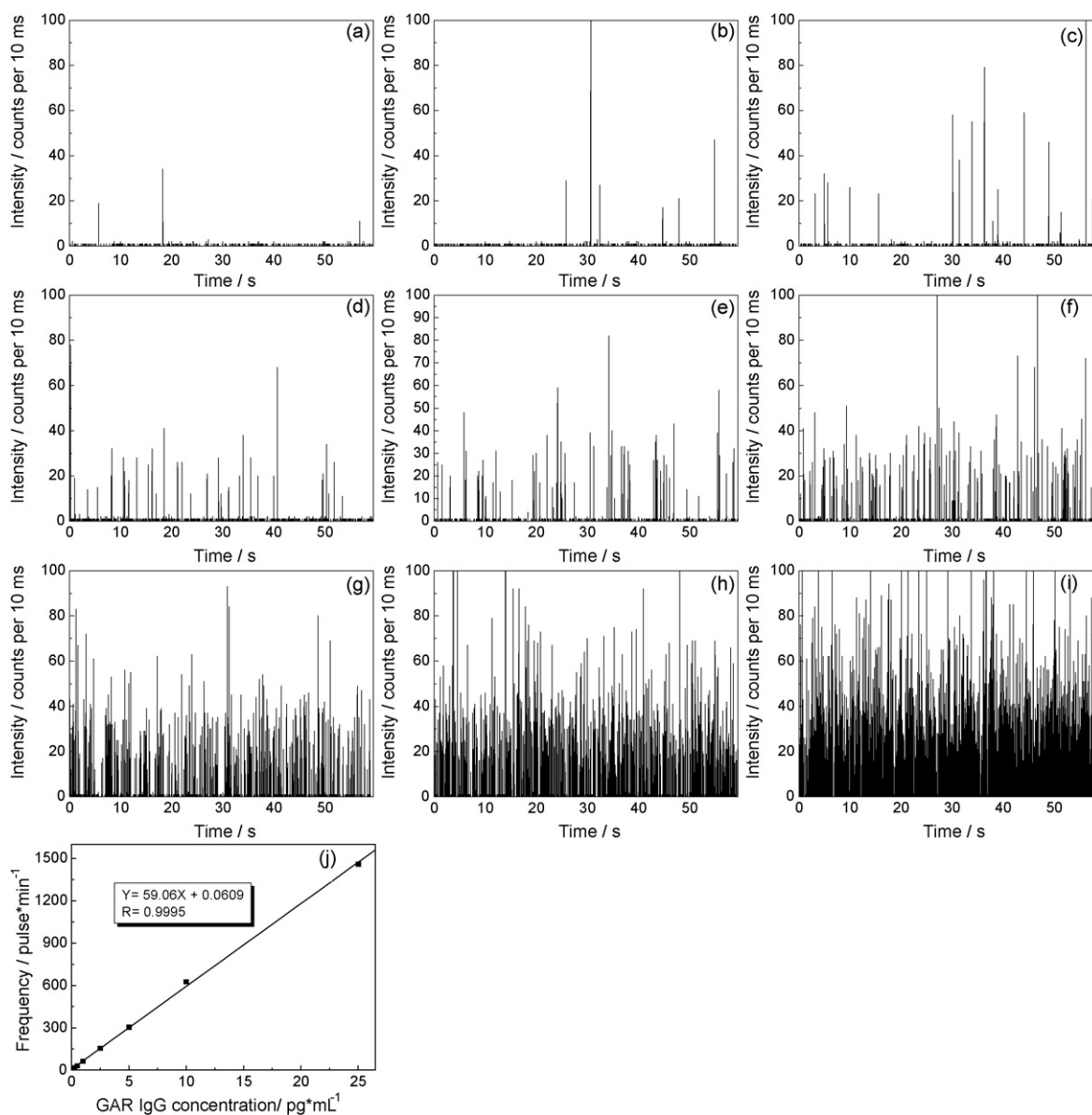


Fig. 4. Transient signals obtained from Au-NPs labeled goat-anti-rabbit IgG (average Au particle size of 45 nm in diameter) with different concentrations by ICP-MS in TRA mode. (a) 10^8 times dilution of the stock solution (0.05 pg mL^{-1} GAR IgG); (b) 5×10^7 times dilution (0.10 pg mL^{-1} GAR IgG); (c) 2×10^7 times dilution (0.25 pg mL^{-1} GAR IgG); (d) 10^7 times dilution (0.50 pg mL^{-1} GAR IgG); (e) 5×10^6 times dilution (1.0 pg mL^{-1} GAR IgG); (f) 2×10^6 times dilution (2.5 pg mL^{-1} GAR IgG); (g) 10^6 times dilution (5.0 pg mL^{-1} GAR IgG); (h) 5×10^5 times dilution (10 pg mL^{-1} GAR IgG); (i) 2×10^5 times dilution (25 pg mL^{-1} GAR IgG); and (j) the plot between the pulse frequency and GAR IgG concentration. Dwell time 10 ms; duration time: 60 s.

our previous research [29]. Au-NPs tend to aggregate under the conditions of acidic media due to hydrogen-bonding [36], though proteins coated over the surface of Au-NPs could alleviate this aggregation. In this case, two dissociating procedures, namely,

15 min shaking after adding 1% HNO_3 solution and 15 min sonication after adding pure water, were compared for the single particle mode immunoassay. The procedure of sonication in pure water exhibited better performance since effective dissociation of Au-NPs

Table 2

Analytical figures for the determination of Au-labeled IgG using different detection modes.

Parameter	ICP-MS detection modes	
	Conventional integral mode	Single particle mode
Sample volume (mL)	0.5	0.8
Calibration function	$I (\text{Signal intensity, cps}) = 28.46C (\text{Au-labeled IgG concentration, pg mL}^{-1}) - 0.41$	$I (\text{Frequency of signal pulse}) = 59.06C (\text{GAR IgG concentration, pg mL}^{-1}) + 0.06$
Correlation coefficient (R)	0.9995	0.9995
Detection limit of Au-labeled IgG (pg mL^{-1})	0.2	0.02
Linear range of Au-labeled IgG (pg mL^{-1})	0.2–500 ^a	0.02–25
Precision (RSD, %)	5.6 (25 pg L^{-1} , $n = 3$)	6.9 (2.5 pg mL^{-1} , $n = 3$)

^a The maximum concentration studied.

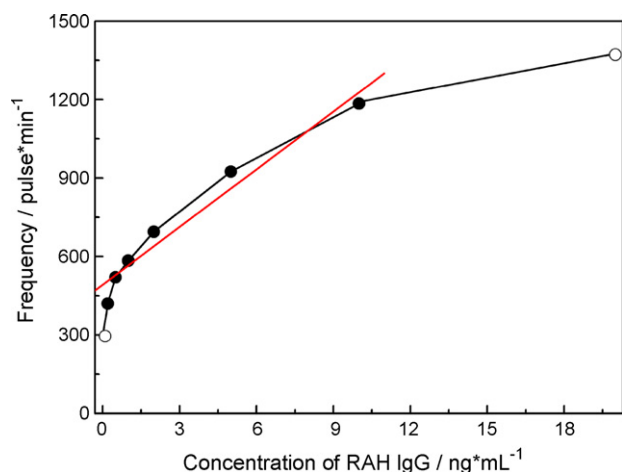


Fig. 5. Dependence of Au-NPs frequency on rabbit-anti-human IgG concentration. Dwell time 10 ms; duration time: 60 s; Au-NPs labels dilution rate: 1:40.

from the complex as well as no extraordinarily high transient signal, while HNO_3 procedure showed the deficiency in partial aggregation of Au-NPs and relatively higher blank noise.

During the sandwich immunoassay, the dilution rate of Au-NPs labeled antibody is a key factor affecting the detection sensitivity and the unspecific binding of Au-NPs labels [37]. Au-NPs labels in high concentration are usually used to provide high sensitivity for the high concentration range of analyte. However, nonspecific binding of Au-NPs mainly derived from charge attraction, hydrophobic absorption and dative binding is increased accordingly with the increase of Au-NPs labels concentration. The choice of dilution rate of Au-NPs labels should compromise the two aspects of sensitivity and nonspecific binding in order to obtain a favorable detection limit and calibration linear range [15]. In this work, preliminary study was carried out with 1:10, 1:20 and 1:40 dilutions of Au-NPs labels for the single particle mode immunoassay. The signal frequency was comparable with these three dilutions for the detection of 1–10 ng mL^{-1} RAH IgG, while the lowest blank signal was obtained with 1:40 dilution.

3.4. Method validation

Finally, the dependence of Au-NPs frequency on RAH IgG concentration was studied with 1:40 dilution of Au-NPs labels, as

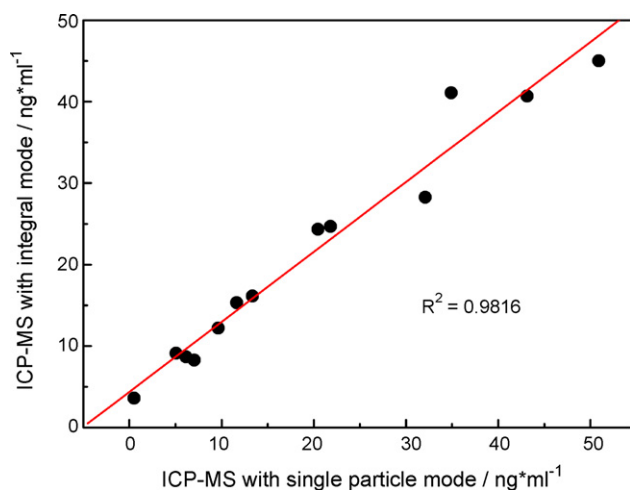


Fig. 6. Correlation of results obtained by conventional integral mode ICP-MS and single particle mode ICP-MS for the determination of rabbit-anti-human IgG.

Table 3
Analytical results of rabbit-anti-human IgG serum samples.

Sample	This method ^a (single particle mode) (ng mL^{-1})	ELISA ^a (ng mL^{-1})
Serum 1	2.4 ± 0.2	2.4 ± 0.1
Serum 2	2.5 ± 0.3	2.8 ± 0.3
Serum 3	5.0 ± 0.4	5.1 ± 0.3
Serum 4	5.4 ± 0.3	5.8 ± 0.6
Serum 5	11.0 ± 1.4	10.6 ± 0.6
Serum 6	10.9 ± 1.2	11.9 ± 0.9

^a Obtained value \pm standard deviation.

shown in Fig. 5. The detection limit of RAH IgG was calculated to be 0.1 ng mL^{-1} (3σ). The calibration graph was linear in the concentration range of $0.3\text{--}10 \text{ ng mL}^{-1}$ ($R^2 = 0.9581$). The departure from linearity was observed when the concentration of RAH IgG was up to 20 ng mL^{-1} . The relative standard deviation (RSD) for three replicate measurements of 2.0 ng mL^{-1} RAH IgG was 8.1%.

In order to verify the accuracy of the proposed method, correlation of results for spiked RAH IgG samples obtained by conventional integral mode ICP-MS and single particle mode ICP-MS was investigated. The results of comparative studies were shown in Fig. 6. It can be seen that relatively good correlation was obtained ($R^2 = 0.9816$) between these two detection modes. To further verify the accuracy of the proposed method, RAH IgG serum samples were also analyzed. The results were shown in Table 3. Results of the proposed method agreed well with those obtained by ELISA, indicating that the present method could be applied to real sample matrices.

4. Conclusion

We have described a sensitive single particle mode ICP-MS sandwich immunoassay for rabbit-anti-human IgG. The comparison of conventional integral mode and single particle mode for the determination of Au-NPs labels demonstrated the good analyzing ability of single particle mode analysis. This highly sensitive method may have many potential applications in biological and clinical analysis. Further work of multiplexing immunoassay based on single particle mode analysis may provide more favorable results with ICP-multicollector-MS or ICP-time of flight-MS. The improvement of instrument detection ability to enable smaller nanoparticle detection is also expected.

Acknowledgments

This work is supported by grants from the Innovation Method Fund of China (No. 2008IM040600) and NSFC (Nos. 20875053 and 20535020).

References

- [1] A. Prange, D. Proefrock, *J. Anal. At. Spectrom.* 23 (2008) 432–459.
- [2] A. Sanz-Medel, M. Montes-Bayon, M. de la Campa, J.R. Encinar, J. Bettmer, *Anal. Bioanal. Chem.* 390 (2008) 3–16.
- [3] J.S. Becker, N. Jakubowski, *Chem. Soc. Rev.* 38 (2009) 1969–1983.
- [4] M. Careri, L. Elviri, A. Mangia, *Anal. Bioanal. Chem.* 393 (2009) 57–61.
- [5] M. Wang, W.Y. Feng, Y.L. Zhao, Z.F. Chai, *Mass Spectrom. Rev.* 29 (2010) 326–348.
- [6] A.P. Deng, H.T. Liu, S.J. Jiang, H.J. Huang, C.W. Ong, *Anal. Chim. Acta* 472 (2002) 55–61.
- [7] D. Iwahata, K. Hirayama, H. Miyano, *J. Anal. At. Spectrom.* 23 (2008) 1063–1067.
- [8] V.I. Baranov, Z. Quinn, D.R. Bandura, S.D. Tanner, *Anal. Chem.* 74 (2002) 1629–1636.
- [9] N. Jakubowski, L. Waentig, H. Hayen, A. Venkatachalam, A. von Bohlen, P.H. Roos, A. Manz, *J. Anal. At. Spectrom.* 23 (2008) 1497–1507.
- [10] M. Careri, L. Elviri, M. Maffini, A. Mangia, C. Mucchino, M. Terenghi, *Rapid Commun. Mass Spectrom.* 22 (2008) 807–811.
- [11] D.J. Kutscher, M.E.D. Busto, N. Zinn, A. Sanz-Medel, J. Bettmer, *J. Anal. At. Spectrom.* 23 (2008) 1359–1364.
- [12] C. Zhang, F.B. Wu, Y.Y. Zhang, X. Wang, X.R. Zhang, *J. Anal. At. Spectrom.* 16 (2001) 1393–1396.

- [13] C. Zhang, F.B. Wu, X.R. Zhang, *J. Anal. At. Spectrom.* 17 (2002) 1304–1307.
- [14] C. Zhang, Z.Y. Zhang, B.B. Yu, J.J. Shi, X.R. Zhang, *Anal. Chem.* 74 (2002) 96–99.
- [15] Y.Y. Lu, W.J. Wang, Z. Xing, S.D. Wang, P. Cao, S.C. Zhang, X.R. Zhang, *Talanta* 78 (2009) 869–873.
- [16] Y.F. Guo, M. Xu, L.M. Yang, Q.Q. Wang, *J. Anal. At. Spectrom.* (2009), doi:10.1039/b902241d.
- [17] A. Merkoci, M. Aldavert, G. Tarrason, R. Eritja, S. Alegret, *Anal. Chem.* 77 (2005) 6500–6503.
- [18] F. Li, Q. Zhao, C.A. Wang, X.F. Lu, X.F. Li, X.C. Le, *Anal. Chem.* 82 (2010) 3399–3403.
- [19] S.D. Tanner, D.R. Bandura, O. Ornatsky, V.I. Baranov, M. Nitz, M.A. Winnik, *Pure Appl. Chem.* 80 (2008) 2627–2641.
- [20] D.R. Bandura, V.I. Baranov, O.I. Ornatsky, A. Antonov, R. Kinach, X.D. Lou, S. Pavlov, S. Vorobiev, J.E. Dick, S.D. Tanner, *Anal. Chem.* 81 (2009) 6813–6822.
- [21] G. Koellensperger, M. Groeger, D. Zinkl, P. Petzelbauer, S. Hann, *J. Anal. At. Spectrom.* 24 (2009) 97–102.
- [22] O.I. Ornatsky, R. Kinach, D.R. Bandura, X. Lou, S.D. Tanner, V.I. Baranov, M. Nitz, M.A. Winnik, *J. Anal. At. Spectrom.* 23 (2008) 463–469.
- [23] S.C. Zhang, C. Zhang, Z. Xing, X.R. Zhang, *Clin. Chem.* 50 (2004) 1214–1221.
- [24] R. Wilson, D.G. Spiller, I.A. Prior, K.J. Veltkamp, A. Hutchinson, *ACS Nano* 1 (2007) 487–493.
- [25] R.W. Hutchinson, A.G. Cox, C.W. McLeod, P.S. Marshall, A. Harper, E.L. Dawson, D.R. Howlett, *Anal. Biochem.* 346 (2005) 225–233.
- [26] J. Seuma, J. Bunch, A. Cox, C. McLeod, J. Bell, C. Murray, *Proteomics* 8 (2008) 3775–3784.
- [27] L. Waentig, P.H. Roos, N. Jakubowski, *J. Anal. At. Spectrom.* (2009) 924–933.
- [28] S.D. Muller, R.A. Diaz-Bobe, J. Felix, W. Goedecke, *J. Anal. At. Spectrom.* 20 (2005) 907–911.
- [29] S. Hu, R. Liu, S. Zhang, Z. Huang, Z. Xing, X. Zhang, *J. Am. Soc. Mass Spectrom.* 20 (2009) 1096–1103.
- [30] C. Degueldre, P.Y. Favarger, S. Wold, *Anal. Chim. Acta* 555 (2006) 263–268.
- [31] U.B. Nielsen, B.H. Geierstanger, *J. Immunol. Methods* 290 (2004) 107–120.
- [32] S.F. Kingsmore, *Nat. Rev. Drug Discov.* 5 (2006) 310–320.
- [33] A.P. Fan, C.W. Lau, J.Z. Lu, *Anal. Chem.* 77 (2005) 3238–3242.
- [34] Z.F. Fu, H. Liu, H.X. Ju, *Anal. Chem.* 78 (2006) 6999–7005.
- [35] A. Clerico, S. Del Ry, D. Giannesi, *Clin. Chem.* 46 (2000) 1529–1534.
- [36] M.C. Daniel, D. Astruc, *Chem. Rev.* 104 (2004) 293–346.
- [37] J. Gu, M. Dandrea, *Am. J. Anat.* 185 (1989) 264–270.